CIAMTIS

U.S. DOT Region 3 University Transportation Center

Finite Element Model Updating for Bridge Deformation Measurements Extracted from Remote Sensing Data

March 9, 2021

Prepared by:

D. Lattanzi

George Mason University

r3utc.psu.edu

PennState College of Engineering

LARSON TRANSPORTATION INSTITUTE

DISCLAIMER

Technical Report Documentation Page

1. Report No.	2. Government Accession No.	3. Recipient's Catalog No.
CIAM-COR-R02		

4. Title and Subtitle	5. Report Date
Finite Element Model Updating for Bridge Deformation Measurements Extracted from Remote Sensing Data	March 9, 2021
	6. Performing Organization Code

7. Author(s)	8. Performing Organization Report No.
David Lattanzi https://orcid.org/0000-0001-9247-0680	

9. Performing Organization Name and Address	10. Work Unit No. (TRAIS)
George Mason University 4400 University Drive Fairfax, VA 22030	**11. Contract or Grant No.** 69A3551847103

12. Sponsoring Agency Name and Address	13. Type of Report and Period Covered
U.S. Department of Transportation Research and Innovative Technology Administration 3rd Fl, East Bldg E33-461 1200 New Jersey Ave, SE Washington, DC 20590	Final Report 3/11/2019 – 3/31/2021
	14. Sponsoring Agency Code

15. Supplementary Notes

Work funded through The Pennsylvania State University via the University Transportation Center Grant Agreement, Grant No. 69A3551847103.

16. Abstract

The objective of the research project was to develop and implement a procedure for transforming point clouds into inputs for finite element analysis. While methods exist for quantifying 3D deformations from point cloud data, they have not been sufficiently evaluated, and the resulting information cannot be leveraged for FEA due to the unstructured nature of the data and complex noise characteristics. More importantly, the resulting scalar field measurements of deformation are not locally smooth and therefore create numerical instabilities when directly mapped to FEA. The purpose of this project was to develop an analytical pathway that addresses these problems, enables new uses for remote sensing, and provides a basis for rapid and quantitative structural capacity in a manner that currently does not exist.

17. Key Words	18. Distribution Statement
Condition assessment, transportation structure, nondestructive evaluation, point cloud, 3D deformation, remote sensing, finite element analysis	No restrictions. This document is available from the National Technical Information Service, Springfield, VA 22161

19. Security Classif. (of this report)	20. Security Classif. (of this page)	21. No. of Pages	22. Price
Unclassified	Unclassified	18	

TABLE OF CONTENTS

LIST OF FIGURES

LIST OF TABLES

CHAPTER 1

Introduction

BACKGROUND

Accurate and rapid condition assessment of in-service transportation structures is critical for system-wide prioritization decisions. These routine assessments require evaluating a given structure for a variety of defects and aging phenomena, in particular changes in the geometric configuration such as plastic deformations or changes in bearing rotational restraint. Such defects have a direct impact on structural capacity and long-term serviceability. While accurate and quantitative geometric measurements are extremely valuable, they are impractical to collect and leverage using conventional condition assessment methods. In response, three-dimensional (3D) remote sensing has seen expanded interest for the nondestructive evaluation (NDE) of geometric changes, due to the flexibility and improving measurement accuracy of these technologies.

There are several methods to generate dense 3D scans or "point clouds," including Light Detection And Ranging (LiDAR) and photogrammetry, the process of taking measurements from images [1]. The growing maturity of both of these technologies makes them capable of generating photorealistic and scale-accurate 3D models of bridges with accuracy on the millimeter scale, sufficient for many inspection and evaluation applications. These 3D representations of arbitrary in-situ conditions can currently be used for measurements, volumetric estimation, and change detection [2]–[4]. In most applications, defects are identified by comparing a 3D scan of a damaged structure against a scan taken prior to damage onset. Ideally these defects are then translated into an update of a finite element analysis (FEA) model of a structure, for quantitative asset management. Such algorithms would directly support load rating and long-term condition assessment practices by enabling quantitative capacity assessments while providing a foundation for asset owners to make data-driven decisions and prognoses of vulnerable assets.

FEA solvers require deformation measurement fields that are locally smooth and, ideally, that provide some quantification of measurement uncertainty (UQ) for statistical analysis. The difficulty is that point-wise defect measurements do not explicitly meet either of these criteria, presenting numerical difficulties for FEA applications. This has limited the application of remote sensing to FEA and infrastructure asset management [5]–[7].

OBJECTIVES

The objective of the research project was to develop and implement a procedure for transforming point clouds into inputs for finite element analysis. While methods exist for quantifying 3D deformations from point cloud data [8], they have not been sufficiently evaluated, and the resulting information cannot be leveraged for FEA due to the unstructured nature of the data and complex noise characteristics. More importantly, the resulting scalar field measurements of deformation are not locally smooth and therefore create numerical instabilities when directly mapped to FEA [7]. The purpose of this project was to develop an analytical pathway that addresses these problems, enables new uses for remote sensing, and provides a basis for rapid and quantitative structural capacity in a manner that currently does not exist.

Specific Sub-objectives

1. The development of a robust 3D deformation measurement approach applicable to large-scale infrastructure systems;
2. The creation of a process for mapping deformation measurements into a form suitable for finite element analysis;
3. Quantification of measurement uncertainty in a manner that supports rigorous statistical analysis; and
4. Experimental validation of all algorithms.

RESEARCH PRODUCTS

Data and Programming Scripts

This project resulted in a variety of data types, as delineated in the Center's data management plan. Experimental data were generated and were stored in comma-delimited text files for dissemination and data transfer. The majority of these files were images and 3D point clouds of experimental specimens. Analytical and numerical code was written in both the R and Python programming languages, and is stored as open-source scripting files. A significant portion of this code base was optimized for general processing unit (GPU) acceleration. All data will be deposited in the Center's data repository within 30 days after submission of this report. The research team did not collect any personally identifiable information (PII), confidential business information, or national security information as a result of this work.

Other Research Products

The research project also resulted in several other products. The work is associated with two conference publications and one additional conference presentation. Unfortunately, COVID-19 caused the cancellation of these conferences and delayed publication until the fall of 2021 and spring of 2022. The work has also resulted in a journal manuscript, to be submitted for publication in the summer of 2021. Two graduate students and one undergraduate student were supported by this research effort.

CHAPTER 2

Methodology

INTRODUCTION

This research project required 5 main tasks:

1. Literature review
2. Development of an approach to measuring structural deformations in point clouds
3. Development of an approach for transforming point cloud measurements for finite element analysis
4. Integration of uncertainty quantification (UQ) measures
5. Experimental evaluation of all tested processes

PROJECT TASKS

Task 1: Literature Review Findings

As TLS and photogrammetric 3D reconstruction methods continue to improve with respect to their size, accuracy, and cost, researchers continue to expand and improve the use of point clouds across a range of engineering and scientific disciplines. Within the context of structural engineering, researchers have used point cloud data to support such activities as structural health monitoring and finite element model updating. Common uses of point clouds for structural health monitoring include deformation tracking and damage detection. Deformation measurement studies have been performed under a range of laboratory and field conditions [4], [6]. Other work has demonstrated the fusion between TLS and photogrammetry point cloud data for enhanced measurement accuracy [9]. Generally speaking, the measurement accuracy of these methods is, at the time of this report, approximately on the scale of one millimeter of deformation. For damage detection, researchers have done work with point cloud analysis to find cracks and detect corrosion [10]–[12]. There have also been studies showing the effectiveness for capturing defects in water resource infrastructure [13], [14]. There are also several recent studies focused on how to connect point cloud data to mechanics-driven simulation models, in particular finite element analysis. The majority of these studies have investigated applications in heritage (historical) structural analysis and rehabilitation [15]–[17].

Despite these uses of point clouds in research and commercial applications, many challenges remain including the handling of varying point densities within a point cloud. Defined as the number of collected data points per unit area of the point cloud, these varying densities occur due to the changing range and incidence angle from the scanner to the target object in the case of TLS collection, and they occur as a result of the feature mapping process in photogrammetry. This problem creates challenges with point set registration, a key step in most point cloud analysis methods, particularly for deformation quantification. The varied densities make it difficult for registration algorithms to correctly align overlapping portions of point clouds when creating large point clouds from the conglomeration of smaller ones. Also, because

features of point cloud data are typically dependent on local neighborhood size, varied densities can lead to other challenges when conducting feature extraction. With respect to surface representation, many point cloud work flows create meshes of the point cloud data for further analysis (in finite element models, for example), and the varied point density across the surface of the point cloud contributes to unquantified uncertainties. These challenges have led to a body of research aimed at dealing with this problem. Some researchers have attempted to use machine learning to address this issue, or more general statistical estimation and fitting methods [18], [19].

Overall, there is minimal work on dealing with varied point densities in image-based collection techniques such as photogrammetry or videogrammetry, and addressing this issue is fundamental to using point clouds in FEA. In most cases, the point clouds in these image-based techniques are more unstructured than the TLS-based techniques. It is also worth pointing out that the prior research cited in regard to handling varied point densities does not create uniformly gridded point clouds, but only improves the original point clouds by decreasing the variance in point cloud density across the target. Thus, as analysis continues after implementing these techniques, the problems with registration, feature extraction, and surface representation persist, albeit at a lesser degree.

Focus of this study

Based on the findings of this literature review, the research team focused on developing algorithmic solutions to the challenges of transforming irregularly spaced point clouds into a format that reduces numerical issues with the FEA process, and that enables explicit uncertainty quantification. This last aspect was found to be a key research gap, as the ability to quantify measurement uncertainty is important for modern statistical approaches to FEA and associated risk analysis protocols.

Algorithm development

The overall algorithmic process developed under this research project is shown in Figure 1. First, point clouds are generated from a collection of images using a photogrammetric structure-from-motion process (SfM). In SfM, sparse point clouds are first generated, followed by a computer vision process that increases the density of the point cloud by several orders of magnitude. Local neighborhoods of points are defined for a given point set, defining the statistical basis region for each point in the cloud. The points are then interpolated onto a 3D grid in a manner that provides local smoothness in subsequent deformation quantification and finite element model updating procedures.

Initially, the research team considered the possibility of computing the deformations prior to interpolation. However, by interpolating prior to deformation quantification, the point clouds are effectively smoothed and denoised. This has the carry-on effect of reducing measurement variances and error, and it eliminated the need for more complex and noise-invariant deformation quantification methods.

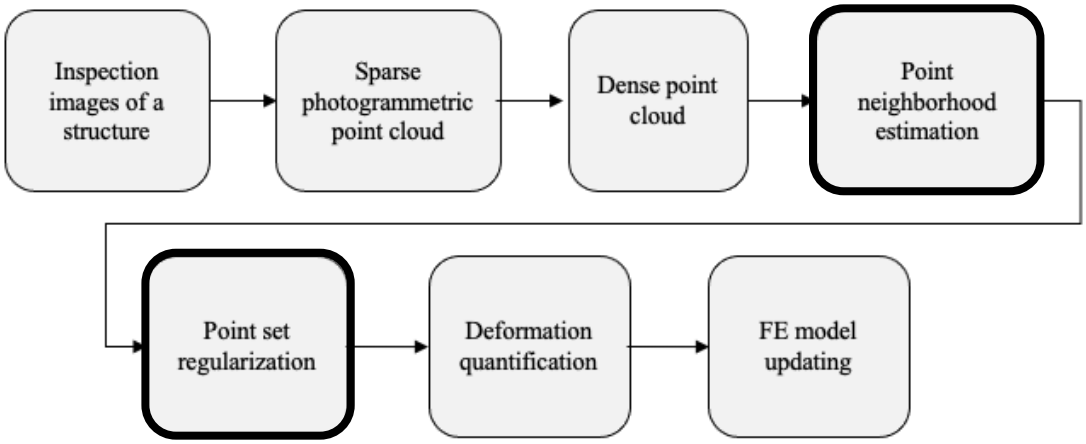

Figure 1. Analytical workflow for point cloud transformation. Bolded components indicate the focus of this research project.

Task 2: Deformation Quantification

Upon completion of the literature review, the first task was to establish a deformation quantification process that was robust to the localized measurement noise endemic to remote sensing data. Conventional deformation measurements compute the 3D Hausdorff distance [8]. When used to compare two point clouds, the Hausdorff distance can be thought of as a point-to-point Euclidean measure of geometric deformation. Through preliminary experiments, this process was found to be highly susceptible to distortional noise. A variety of deformation measurement approaches were tested and considered throughout the project. Ultimately, the research team decided to consider the idea of smoothing and regularizing the point clouds prior to deformation quantification. The kriging process developed under Task 3 to regularize the point grid has the added benefit of denoising the point sets and addressed many of the issues with measurement noise considered in Task 2. This enabled the use of standard Hausdorff distance for deformation measurement without the need for more complex deformation measures that often are accompanied by empirical tuning parameters.

This finding changed the course of the research project significantly and placed the majority of the research focus on Task 3 as a result. Additional consideration of Task 2 objectives related to deformation quantification metrics and algorithms are now considered a potential avenue for future research.

Task 3: Point Cloud Transformation

This task was focused on how to transform raw, unstructured point clouds into a regularized 3D gridded data set (voxelization) that maintained local smoothness for finite element model updating. The focus of the task was on Gaussian kriging, a process that has seen use for statistical smoothing and uncertainty quantification [20]. Kriging allows for the prediction of deformation values at locations without observations (i.e., at locations between the data points from the point cloud) based on statistical likelihood analysis. This enables the ability to define the grid to any desired point cloud density, a significant benefit for FEM updating.

Kriging, also known as Gaussian process regression, is a technique that uses a Gaussian process model to make predictions of some property at unobserved locations based on the spatial covariances and values of

the observed data within a local neighborhood of similar values. In the context of this work, it was identified as a process that could serve to regularize 3D point clouds (Task 3) and provide uncertainty quantification about those measurements (Task 4). In broad terms, kriging uses a weighted average of nearby observations when determining the expected values of a given property at prediction locations. This process operates under the idea that closer observations to the prediction location should have higher weights than observations that are farther away. As other techniques such as inverse distance weighting [21] follow this same idea, kriging is unique in its calculation of these weights through the spatially based covariance relationship of the observations. This covariance relationship also serves as an explicit, centrality-based estimate of measurement uncertainty.

Given observations of a property (3D deformations in this case) within a local neighborhood, *kriging* assumes that the value of an observation can be represented as a Gaussian observation, with an expected mean value and estimation of the error represented as a covariance. Achieving this requires a representation of the error over a local neighborhood. In *ordinary kriging*, the mean measurement value is assumed constant over the neighborhood. *Universal kriging* permits variation in the mean measurement, and in this work the mean was expressed as a generalized linear model of the spatial coordinates. Both kriging processes were considered in this work. For more details on kriging, the reader is referred to [20].

These kriging processes were used to take the 3D deformation measurements described previously and then interpolate them onto a regularized 3D grid, which was the primary goal of the project. However, an added benefit of this process is that the statistical nature of kriging provides a locally smooth denoising of observations and improves the deformation estimation process described in Task 2. Additionally, the inherent nature of kriging means that UQ is performed with respect to Gaussian representations of mean and covariance. These values can be directly applied to statistical risk analysis.

Task 4: Uncertainty Quantification

The quantification of measurement uncertainty in the deformation measurements ultimately provides the basis for statistical analysis by stakeholders and engineers performing risk analysis based on remote sensing data. After UQ, a range of numerical simulations can be performed to identify statistically unlikely, but unacceptably high-risk structural performance degradations. In this work, the kriging process used for point interpolation in Task 3 provided a statistical uncertainty measure, as the Gaussian model used for statistical interpolation provides a centrality-based measure of point set uncertainty. This UQ measure was appended to the standard point cloud data-type (an XYZ-tuple) as an additional scalar field that could be employed for statistical FE updating.

Task 5: Experimental Evaluation

The methodologies developed in Tasks 2-4 were prototyped and validated through a combination of synthetic and laboratory testing. Existing point cloud data available to the PI were used for initial prototyping. There were then a series of follow-on laboratory experiments using laboratory specimens designed to simulate various mechanical deformation profiles, with measurement precision on the order of 0.4 mm. Additional full-scale point set data were made available through collaborations on other CIAMTIS projects. The results of these experiments are shown in Chapter 3.

CHAPTER 3

Findings

EXPERIMENTAL DESIGN

To study the feasibility of the algorithmic process, in particular the kriging methods developed under Task 3, a series of experimental tests were performed. While a variety of preliminary experiments were performed, the focus was on a series of controlled laboratory experiments designed to evaluate the measurement accuracy of the kriging process. The experiments were designed to simulate plate deformations in a structural component, and the analysis of the associate point clouds.

Test Specimens

Creating controlled mechanical deformations with a highly precise ground truth measurement, particularly when observing 3D field data, is extremely difficult. To simulate this process in a more controlled manner, a series of 3D printed specimens were generated (Figure 2). Each specimen represented a deformed plate with base dimensions of 150 mm x 150 mm. For each of the "deformation surrogates," the third dimension varied from 5 mm to 45 mm to simulate various deformation profiles. The deformation surfaces for these surrogates were defined by a variation of half period [-Π/2, Π/2] cosine functions. All specimens were professionally printed in ABS plastic, with a part accuracy of ±0.375 millimeters. In order to improve the effectiveness of feature mapping during photogrammetry, the 3D printed specimens were spray painted with nonreflective Krylon Stone Coarse Texture black granite spray paint. The painting process added an estimated +0.8 millimeters of thickness to the specimens. This value was estimated based on the mass of paint used for the given surface area of the deformation surrogates, but it is worth noting that it was not possible to apply a perfectly uniform coat of paint nor was it possible to ensure that the paint dried and settled in an even manner when applied to the surface of each deformation surrogate. These variations in paint thickness inevitably played a role in the resulting experimental error.

The purpose of the various deflection patterns was to evaluate the effectiveness of kriging interpolation on a range of deflection geometries and magnitudes. The knowledge of the surface function for each shape,

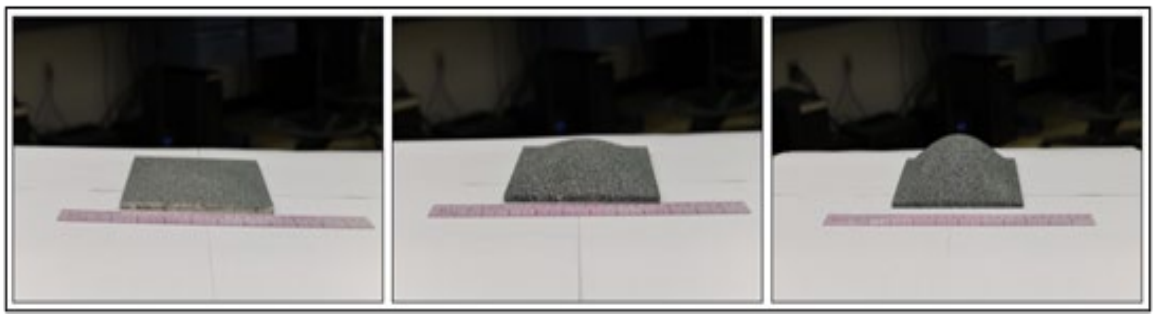

Figure 2. Examples of 3 different specimens printed for experimental evaluation of the kriging interpolation process.

combined with the knowledge of the printer accuracy, enabled the isolation of errors from kriging interpolation when compared to the complex sources of errors that can result from the photogrammetric reconstruction process.

Point Cloud Generation and Analysis

In order to generate point clouds, photogrammetric remote sensing was used. This process initiated with the capture of a set of high-quality images of a specimen. These images were captured under controlled lighting conditions in order to control for environmental variables. Photographs were collected using a 45-megapixel Nikon D850 camera with a 50-millimeter focal length lens. 3D point clouds of each specimen were generated in *Agisoft Metashape*. Scaling and point cloud preprocessing were done in *CloudCompare*.

After a 3D point cloud was generated for each deformation surrogate, the resulting fields were interpolated onto a 3D grid via kriging interpolation. Both ordinary kriging and universal kriging were evaluated. The inverse distance weighting (IDW) algorithm [20]–[22] was also evaluated as a comparative interpolation approach; however, IDW does not provide UQ and therefore was not the focus of this research effort. Two different approaches to local neighborhood estimation, a fundamental step in the kriging process, were evaluated. One approach was based on all points within a 1-mm radius of each point, and one estimator used the 100 nearest neighbors in a point cloud. All interpolative computations were performed in the R programming language. Scripts and data products for this study will be shared per CIAMTIS UTC policies.

RESULTS

The interpolated kriging results were compared against the ground truth specimen dimensions of each surrogate at each interpolated location. An example result from these tests is shown in Table 1 and Figure 3. The results of these experiments indicated that interpolated measurement error for the kriging process was, on average, 0.72 mm when compared to comparisons between the dense point clouds and the functional shape profiles. Differences between ordinary and universal kriging results, as well as with IDW, were negligible. With respect to the comparison of ordinary and universal kriging, the search neighborhood based on the dense cloud and a 1-mm radius shows no difference between the results at the micrometer level, while the search neighborhood based on the dense cloud with 100 nearest neighbors shows differences at the micrometer level in only a couple of cases. While an exhaustive reporting of these findings is beyond the scope of this report, and is the focus of an upcoming journal manuscript, the results indicated that, while the kriging process does induce some measurement error, its impacts are minimal compared to other sources of error in the experimental process, such as those from part fabrication, and error inherent to the photogrammetric reconstruction process. The differences between the various interpolators were found to be negligible when compared to the errors induced by the point cloud generation process itself.

Table 1. Example comparative error analysis (RMSE, units of mm) of kriging and inverse distance weighting interpolators (1-mm radius neighborhood) against ground truth errors from functional shape profiles. Dense cloud refers to a comparison between the uninterpolated point cloud and function profile.

Shape #	Dense Cloud	Ordinary Kriging	Universal Kriging	IDW
1	1.302	1.302	1.302	1.302
2	0.617	0.614	0.614	0.615
3	0.838	0.835	0.835	0.836
4	0.999	0.978	0.978	0.980
5	0.849	0.837	0.837	0.838
6	0.617	0.598	0.598	0.598
7	0.367	0.367	0.367	0.366
8	0.305	0.292	0.292	0.292

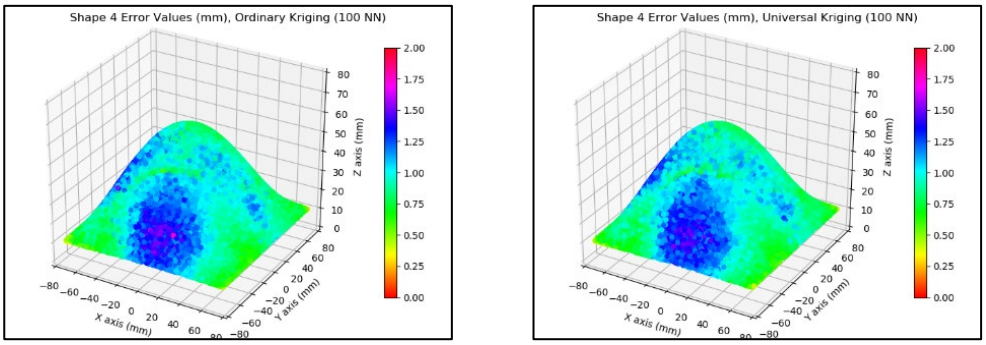

Figure 3: Comparison between ordinary and universal kriging interpolators (1-mm radius point neighborhood). The negligible difference in the results suggests that ordinary kriging is suitable for this task, with lower computational cost as a result.

CHAPTER 4

Recommendations

MAJOR CONCLUSIONS

The purpose of this study was to develop a process for transforming point cloud data into a format that could, in the future, be used for finite element model updating. The core aspect of this process is the statistical interpolation technique of kriging, also known as Gaussian process regression. The kriging process developed in this research program is designed to statistically interpolate a point cloud onto a regular grid in a locally smooth fashion, while simultaneously providing explicit uncertainty quantification of measurement error. The development of this process enables consistent and controllable deformation quantification, with reduced distortional noise due to the inherent smoothing that kriging provides. This approach is agnostic to the method of data collection and can be used just as effectively for point clouds collected by laser scanners as it can be used for photogrammetry- or videogrammetry-based point clouds.

Experimental analysis of this process showed that kriging maintains the accuracy level of the given point cloud that is used for the observations to make predictions of the deformation values at the target locations. Our results indicated that the method of kriging, whether ordinary or universal kriging, did not impact the accuracy of the results within the practical limits of the errors and uncertainties from the registration process of the photogrammetry, the 3D printer accuracy, and the amount of textured paint applied to the surface of the surrogates. We further showed that in practical terms, when conducting kriging of a point cloud (which typically has much higher data density than common applications for kriging) the kriging methods and neighborhood structures that we used had negligible impact on the variance intervals. The variance intervals of the predictions are key, as they become the primary measure of uncertainty quantification.

AVENUES FOR FUTURE WORK

It is important to understand that, despite the promising results of this study, we did not exhaustively explore the effects of data set size, point cloud density, or neighborhood size on kriging accuracy. Future work will look at the relationship between point cloud density of a surface and its effects on errors of kriging predictions. This approach could determine the potential for further subsampling a point cloud below the point density explored in this research to determine if the kriging techniques maintain the accuracy that was presented in this work. Additionally, many resources note that the number of neighbors (observations) required for a given kriging prediction is much lower than the values used in this work. Exploring the minimum neighborhood size required to maintain appropriate accuracy levels, as demonstrated in this work, would provide insight into methods for decreasing the computational expense of this approach. Additional avenues for future work related to this research include its use in finite element model updating, its application to physical infrastructure in a field environment, and its implementation with more advanced registration techniques. The combination of these research tasks will ultimately facilitate the ability to quantify small geometric changes through point cloud analysis, further aiding current methods in such arenas as deformation tracking and structural health monitoring.

IMPLEMENTATION CONSIDERATIONS

It is not anticipated that the results of this work would be directly implemented in practice. Rather, they would likely be implemented as a component of a larger software package of 3D point cloud generation and analysis tools designed for practicing engineers. Such tools are offered by Bentley Systems and Autodesk, as well as the CloudCompare platform. Achieving implementation within these programs would require coordination with the software vendors as well as a more in-depth study regarding user interface considerations.

References

[1] R. Hartley and A. Zisserman, *Multiple view geometry in computer vision*, vol. 2. Cambridge Univ Press, 2000.

[2] K. Ghahremani, A. Khaloo, and D. Lattanzi, "Automated 3D Image-Based Section Loss Detection for Finite Element Model Updating," *ISARC Proc.*, vol. 2016 Proceedings of the 33rd ISARC, Auburn, USA, pp. 403–411, 2016.

[3] A. Khaloo and D. Lattanzi, "Automatic Detection of Structural Deficiencies Using 4D Hue-Assisted Analysis of Color Point Clouds," in *Dynamics of Civil Structures, Volume 2*, Springer, Cham, 2019, pp. 197–205.

[4] B. Jafari, A. Khaloo, and D. Lattanzi, "Deformation Tracking in 3D Point Clouds Via Statistical Sampling of Direct Cloud-to-Cloud Distances," *J. Nondestruct. Eval.*, vol. 36, no. 4, p. 65, Dec. 2017, doi: 10.1007/s10921-017-0444-2.

[5] M. E. Stavroulaki, B. Riveiro, G. A. Drosopoulos, M. Solla, P. Koutsianitis, and G. E. Stavroulakis, "Modelling and strength evaluation of masonry bridges using terrestrial photogrammetry and finite elements," *Adv. Eng. Softw.*, vol. 101, pp. 136–148, Nov. 2016, doi: 10.1016/j.advengsoft.2015.12.007.

[6] Yan Yujie, Guldur Burcu, and Hajjar Jerome F., "Automated Structural Modelling of Bridges from Laser Scanning," *Struct. Congr. 2017*, doi: 10.1061/9780784480403.039.

[7] Ma Ling, Sacks Rafael, Zeibak-Shini Reem, Aryal Ashrant, and Filin Sagi, "Preparation of Synthetic As-Damaged Models for Post-Earthquake BIM Reconstruction Research," *J. Comput. Civ. Eng.*, vol. 30, no. 3, p. 04015032, May 2016, doi: 10.1061/(ASCE)CP.1943-5487.0000500.

[8] D. Lague, N. Brodu, and J. Leroux, "Accurate 3D comparison of complex topography with terrestrial laser scanner: Application to the Rangitikei canyon (N-Z)," *ISPRS J. Photogramm. Remote Sens.*, vol. 82, pp. 10–26, Aug. 2013, doi: 10.1016/j.isprsjprs.2013.04.009.

[9] A. Guarnieri, F. Remondino, and A. Vettore, "Digital photogrammetry and TLS data fusion applied to Cultural Heritage 3D modeling," *Int. Arch. Photogramm. Remote Sens. Spat. Inf. Sci.*, vol. 36, no. 5, pp. 1–6, 2006.

[10] N. Khurram, E. Sasaki, H. Kihira, H. Katsuchi, and H. Yamada, "Analytical demonstrations to assess residual bearing capacities of steel plate girder ends with stiffeners damaged by corrosion," *Struct. Infrastruct. Eng.*, vol. 10, no. 1, pp. 69–79, Jan. 2014, doi: 10.1080/15732479.2012.697904.

[11] B. Riveiro, H. González-Jorge, M. Varela, and D. V. Jáuregui, "Validation of terrestrial laser scanning and photogrammetry techniques for the measurement of vertical underclearance and beam geometry in structural inspection of bridges," *Measurement*, vol. 46, no. 1, pp. 784–794, 2013.

[12] D. F. Laefer, L. Truong-Hong, H. Carr, and M. Singh, "Crack detection limits in unit based masonry with terrestrial laser scanning," *Ndt E Int.*, vol. 62, pp. 66–76, 2014.

[13] D. González-Aguilera, J. Gómez-Lahoz, and J. Sánchez, "A new approach for structural monitoring of large dams with a three-dimensional laser scanner," *Sensors*, vol. 8, no. 9, pp. 5866–5883, 2008.

[14] T. Schäfer, T. Weber, P. Kyrinovic, and M. Zámecniková, "Deformation measurement using terrestrial laser scanning at the hydropower station of Gabcikovo," 2004.

[15] D. V. Jáuregui, Y. Tian, and R. Jiang, "Photogrammetry applications in routine bridge inspection and historic bridge documentation," *Transp. Res. Rec. J. Transp. Res. Board*, vol. 1958, no. 1, pp. 24–32, 2006.

[16] G. Castellazzi, A. M. D'Altri, S. de Miranda, and F. Ubertini, "An innovative numerical modeling strategy for the structural analysis of historical monumental buildings," *Eng. Struct.*, vol. 132, pp. 229–248, 2017.

[17] C. Bertolini-Cestari, S. Invernizzi, A. Spanò, and L. Mallamaci, “Laser modeling and structural assessment of a XVIIth century wooden dome,” *Wiad. Konserw.*, pp. 151–156, 2012.
[18] W. Xu and I. Neumann, “Finite element analysis based on a parametric model by approximating point clouds,” *Remote Sens.*, vol. 12, no. 3, p. 518, 2020.
[19] G. Castellazzi, A. M. D’Altri, G. Bitelli, I. Selvaggi, and A. Lambertini, “From laser scanning to finite element analysis of complex buildings by using a semi-automatic procedure,” *Sensors*, vol. 15, no. 8, pp. 18360–18380, 2015.
[20] M. L. Stein, *Interpolation of Spatial Data: Some Theory for Kriging*. Springer Science & Business Media, 2012.
[21] G. Y. Lu and D. W. Wong, “An adaptive inverse-distance weighting spatial interpolation technique,” *Comput. Geosci.*, vol. 34, no. 9, pp. 1044–1055, 2008.
[22] G. Farin, “A modified Clough-Tocher interpolant,” *Comput. Aided Geom. Des.*, vol. 2, no. 1, pp. 19–27, Sep. 1985, doi: 10.1016/0167-8396(85)90003-2.